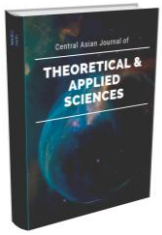

CENTRAL ASIAN JOURNAL OF THEORETICAL AND APPLIED SCIENCE

https://cajotas.casjournal.org/index.php/cajotas

Volume: 07 Issue: 02 | April 2026 ISSN: 2660-5317

Article

Use of Iodine As A Catalyst in The Synthesis and Characterization of Pyrrolidone and Evaluation of Its Biological Activity

Maan Ziadan Khalaf

1. Education of Salah al-Din, Ministry of Education, Iraq

* Correspondence: maanqqqq@gmail.com

Abstract: In this field, several pyrrolidone compounds were created using iodine as a catalyst. The accuracy of the data was confirmed using spectroscopic methods, namely proton and carbon nuclear magnetic resonance (NMR), as well as mass spectrometry, to evaluate their analgesic properties using two contrasting methods: the hot plate test and the acetic acid spasm test. In the hot plate test, the results showed that the control group was unaffected by the analgesic, exhibiting consistent response times. Compound C10 showed a clear treatment of 20 mg/kg, with a treatment response time more than three times greater than the standard 10 mg/kg treatment. The number of spasms decreased to 6.2 ± 0.66 with the 10 mg/kg dose, while in compound C10, spasms were reduced to 10.10 ± 0.41, equivalent to half the pain. These results confirm that compound C10 is a promising candidate for future pain management.

Keywords: pyrrolidone ring, iodine ctalyste, analgesic activity

Citation: Khalaf, M. Z. Use of Iodine As A Catalyst in The Synthesis and Characterization of Pyrrolidone and Evaluation of Its Biological Activity. Central Asian Journal of Theoretical and Applied Science 2026, 7(2), 121-141

Received: 10th Jan 2026
Revised: 21th Feb 2026
Accepted: 14th Mar 2026
Published: 08th Apr 2026

1. Introduction

Bacterial resistance remains a worldwide problem despite the discovery and development of several antibiotic classes throughout the last century. There are currently a few solutions [1]. Although bacterial resistance can be seen as a natural process, the widespread use and, in many cases, abuse of antibacterial agents in the cultivation of domesticated animals has falsely determined an increase in safe strains, increasing the likelihood of antibacterial resistance microorganisms starting from contaminating humans [2]. Microbe-induced illnesses have previously caused an extremely high rate of death worldwide. Fortunately, a variety of natural and synthetic antibiotics have greatly improved human health since penicillin was first introduced as a powerful antibacterial agent in the 1940s [3]. The proliferation of multidrug-resistant microbial strains and the emergence of incurable infections continue to make treating bacterial inspection difficult. The development of both new and ancient opponents of bacterial resistant strains in previous decades has led to a liberal need for new classes of antibacterial agents, despite the market's plenty of chemotherapeutics and antibacterial experts. As demonstrated by the abundance of bioactive chemicals now on the market, the creation of therapeutically useful medications increasingly depends on the usage of heterocyclic structures, many of which include nitrogen. The pyralidone ring has been used to treat a variety of various illnesses due to its strong action against bacteria, fungus, and as an analgesic, anticancer, anti-inflammatory, and anti-inflammatory agent. Its composition of consecutive lactam

groups with nitrogen that create a five-sided ring is responsible for its action. It has been employed as a polymer in nanomaterials and in therapies for various illnesses because of its ease of breakdown.

According to market research conducted in 2013, overall catalyst sales were estimated to be between US$15 billion and US$19 billion per year, with an annual growth rate of 4% to 5%. Additionally, catalysts offer significantly more value to the process of turning raw materials into finished goods like chemicals and fuels. According to studies, the cost of a catalyst only accounts for 0.1% to 1% of the finished product's profit margin, which means that the catalyst sector generates trillions of dollars in value each year. Even if the number of scientific research on catalysts has dramatically increased, indicating a rising capacity to produce stable, effective, and selective catalysts logically, catalyst production is still frequently seen as more of an art than a science. Numerous earlier research have demonstrated the synthesis of pyralidone compounds, but they did not investigate their analgesic properties or incorporate any additional variables into the synthesis processes [4-20]. The goal of this work is to synthesis many pyralidone compounds utilizing an iodine catalyst that is widely available in the market, selective, and capable of electrophilic substitution. The effects of these substances on bacteria, cancer, and inflammation will next be assessed. Proton and carbon nuclear magnetic resonance spectroscopy and mass spectrometry will be used to verify the correctness of the data and determine the structural makeup of the produced molecules.

2. Materials and Method

List of chemicals

Every research chemical used in the experiments was bought from Merck or Cosmo Chem Pvt. Ltd. All solvents, with the exception of LR grade, were dried and refined as required by the literature. Borosil is used to make the glassware required in the reactions. Before being used, all of the glassware was cleaned using acetone and chromic acid.

Table 1. List Of chemicals used for synthesis

Sr. no.	Chemical Name	Supplied by
1.	Glacial Acetic Acid	Cosmo Chem Pvt. Ltd.
2.	cyclohexanone	Cosmo Chem Pvt. Ltd.
3.	Sulphur,	Cosmo Chem Pvt. Ltd.
4.	Ethyl cyano acetate	Cosmo Chem Pvt. Ltd.
5.	piperidine	Cosmo Chem Pvt. Ltd.
6.	ethanol	Merck
7.	aniline	Cosmo Chem Pvt. Ltd.
8.	diethyl acetylene dicarboxylate	Cosmo Chem Pvt. Ltd.
9.	4-chlorobenzaldehyde	Cosmo Chem Pvt. Ltd.
10.	citric acid monohydrate	Cosmo Chem Pvt. Ltd.

List of instruments

Microscopic slides (2 x 7.5 cm) coated with silica-gel-G and pre-coated silica gel strip were used for TLC. Spots were visible when exposed to iodine vapor and UV light. At Cryogen MASS Services in Mumbai, mass spectra were captured using an ESI-MS mass spectrometer. The Bruker Advance-II 400 MHz equipment was used to produce 1HNMR

spectra in DMSO. Chemical shift was quantified in parts per million downfield from tetramethylsilane (TMS), an internal standard at Cryogen NMR Services, Mumbai.

Table 2. List if instruments required for synthesis

Sr. no.	Name of Instrument	Make
1	Magnetic stirrer	Remi 1MLH
2	Mass Spectroscopy	ESI-MS Mass spectrometer
3	NMR Spectroscopy	Bruker Advance-II 400 MHz
4	Microwave reactor	Anton Paar

Synthesis & Characterization

Scheme Of Pyrrolidone

The synthesis of the target compound has been achieved by adopting following synthetic procedure

Step 1- Ethyl 2-Amino -4,5,6,7 Tetrahydro Benzothiopene 3 -Carboxylate

Step 2-Ethyl 4-hydroxy-5-oxo-1,2-diphenyl-2,5-dihydro-1*H*-pyrrole-3-carboxylate

Step 3-

1. *N*-(3-amino-4,5,6,7-tetrahydrobenzo[*b*]thiophen-2-yl)-4-hydroxy-5-oxo-1,2-diphenyl-2,5- dihydro-1*H*-pyrrole-3-carboxamide
2. ethyl 2-(4-hydroxy-5-oxo-1,2-diphenyl-2,5-dihydro-1*H*-pyrrole-3-carboxamido)-4,5,6,7-tetrahydrobenzo[*b*]thiophene-3-carboxylate

Preparation of Ethyl 2-Amino -4,5,6,7 Tetrahydro Benzothiopene 3 -Carboxylate

Chemicals: cyclohexanone, Sulphur, Ethyl cyano acetate, diethyl amine, ethanol

Apparatus: Glass beakers, Magnetic stirrer, water bath, filtration assembly, hot plate etc.

STEP 1

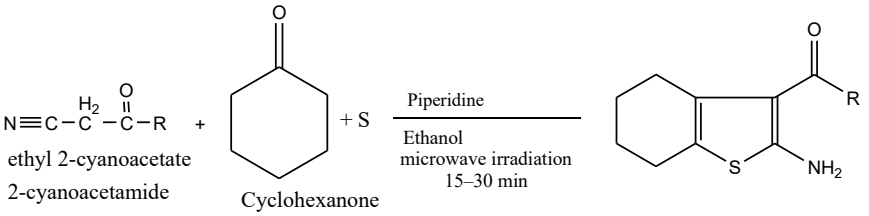

i) 2-amino-4,5,6,7-tetrahydrobenzo[*b*]thiophene-3-carboxamide

ii) ethyl 2-amino-4,5,6,7-tetrahydrobenzo[b]thiophene-3-carboxylate

Step 1 Synthesis

Step-1: In a microwave-safe reaction vessel, a mixture of cyclohexanone (10 mL, 0.1 mol), sulfur (3.2 g, 0.1 mol), ethyl cyanoacetate (10 mL, 0.1 mol), piperidine (15 mL, 0.1 mol), and dry ethanol (20 mL) is irradiated in a microwave reactor at 300–500 W, maintaining a temperature of 80–100°C for 15–30 minutes. After cooling, the reaction mixture is poured into ice-cold water (100–150 mL) with stirring and left undisturbed for 3 hours. The resulting solid is filtered, washed with cold water, and dried at 40–50°C. If needed, the crude product is purified via recrystallization from ethanol-water (3:1). Characterization can be performed using standard techniques like NMR, FTIR, and mass spectrometry.

Step 2:

Chemicals: aniline, diethyl acetylene dicarboxylate, ethanol, 4-chlorobenzaldehyde, citric acid monohydrate

Apparatus:

Glass beakers, Magnetic stirrer, water bath, filtration assembly, hot plate etc

STEP 2

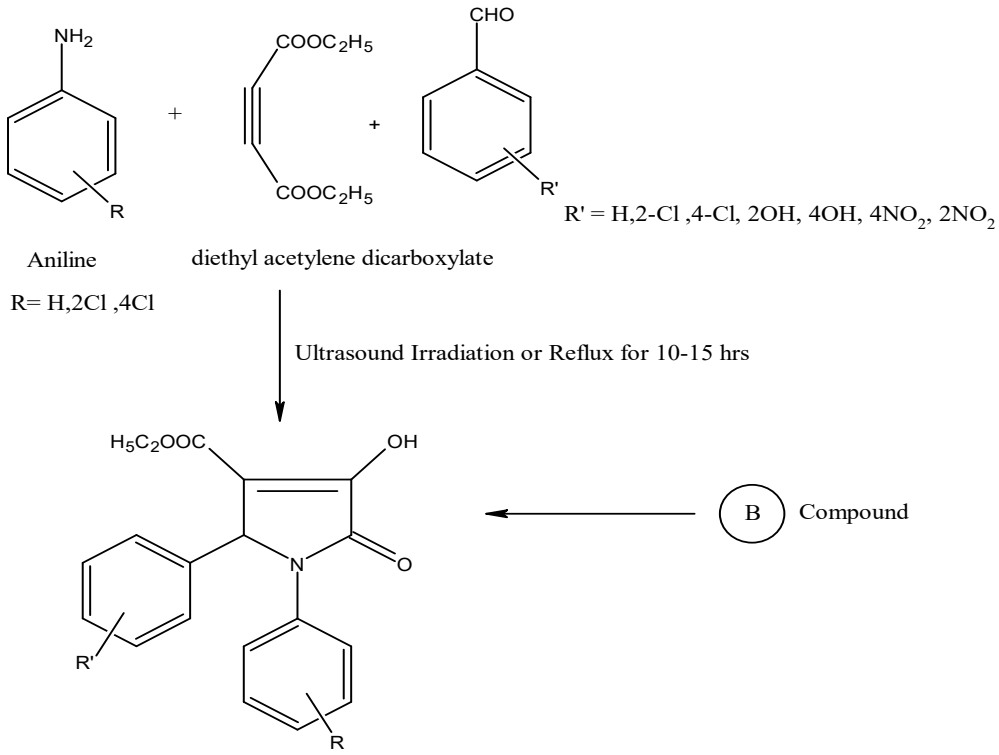

ethyl 4-hydroxy-5-oxo-1,2-diphenyl-2,5-dihydro-1*H*-pyrrole-3-carboxylate

Step 2 Synthesis

Procedure:

Ethanol (4 ml) was mixed with aniline (0.091 ml, 1 mmol) and diethyl acetylenedicarboxylate (0.160 ml, 1 mmol), and the mixture was magnetically stirred at room temperature. After adding 4-chlorobenzaldehyde (0.141 g, 1 mmol) and citric acid monohydrate (0.42 g, 2 mmol), the mixture was subjected to ultrasonic irradiation. The same procedure was also performed without sonication at room temperature. The progress of the reactions (n-hexane: EtOAc, 10:7) was tracked using TLC. The solid product was filtered once the reactions were finished, and the pure product was created by recrystallizing hot ethanol.

Step 3:

Chemicals:

Glacial Acetic Acid, ethanol

Apparatus:

Glass beakers, Magnetic stirrer, water bath, filtration assembly, hot plate etc.

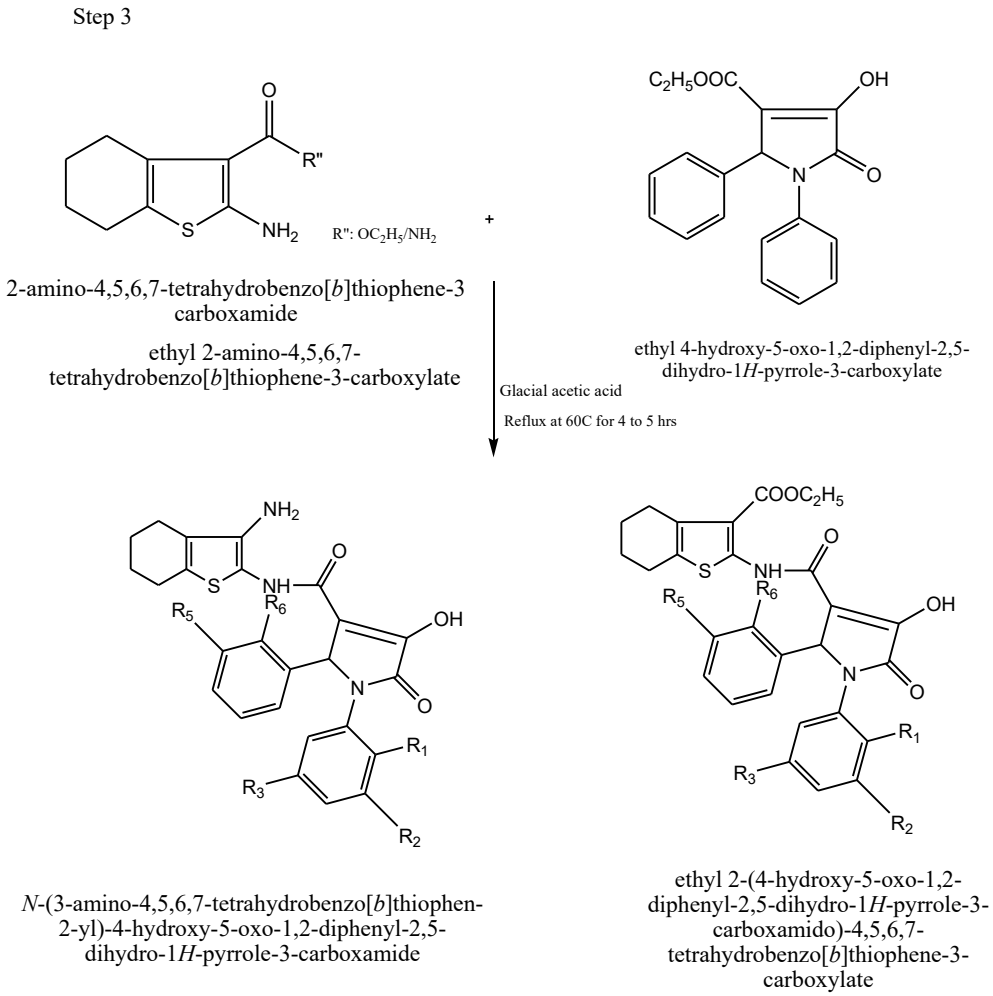

Step 3 Synthesis

Step 3: A compound (0.01 mol) and B compound (0.01 mol) were refluxed in 50 ml of glacial acetic acid at 60C for four to five hours. The reaction mixture was distilled at low pressure in order to remove excess acetic acid by evaporation. The yellow residue was filtered, dried, and recrystallized from ethanol to produce crystalline products [21–25].

Biological Activity

Analgesic activity

Hot plate Method

The analgesic effects of compound 10 (C10) in the central and peripheral nerve systems were assessed in albino male mice using the hot plate test and the acetic acid-induced writhing test, respectively. Hot plate test The hot plate test was carried out in the manner previously mentioned. For this investigation, adult male Albino mice weighing between 20 and 25 grams were chosen. The mice were placed on the heated plate before the experiment. The temperature of the heated plate was maintained at 55 ± 0.5 °C. The latent response was defined as the interval between the placement and the animals' shaking, licking of their rear paws, or leaping reaction.Mice that displayed latencies within five to thirty seconds were selected for the experiment. The selected mice were randomly divided into five groups of eight. The pre-treatment reaction time of each mouse was recorded. Three oral doses of compound 10 (C10) (0.8, 2.4, and 7.2 g/kg, p.o.), the control vehicle (distilled water, 20 mL/kg, p.o.), and the ASA positive control (100 mg/kg, p.o.) were administered for six consecutive days.Each animal's post-treatment response time was measured after 30, 60, 90, and 120 minutes on day 7, one hour after oral delivery. To prevent mouse foot scorching, the cut-off period was set at 60 seconds if the pain domain values were more than 60 seconds.

The percentage inhibition was calculated by using the following formula:

%Inhibition = [(Post-treatment Latency) − (Pre-treatment Latency)]/Pre-treatment Latency × 100.

Acetic acid-induced abdominal writhing in mice

The writhing research test was carried out as previously mentioned. Five treatment groups of eight mice each were randomly assigned to the mice: Three doses of compound 10 (C10) (0.8, 2.4, and 7.2 g/kg, p.o.), vehicle control (distilled water, 20 mL/kg, p.o.), and ASA positive control (100 mg/kg, p.o.). These treatments were administered orally for six consecutive days. On day 7, an hour after oral administration, the mice received an intraperitoneal injection of 10 mL/kg of a 0.6% acetic acid solution in normal saline to cause writhing. The frequency of writhing (pelvic rotation, hind limb stretching, and abdominal constrictions) was recorded for fifteen minutes. Furthermore, the latent phase—the initial period of writhing after an injection of acetic acid—was seen.

The following formula was used to determine the proportion of analgesic activity: %Inhibition is calculated as [numbers of writhes (control) − numbers of writhes (test)]/numbers of writhes (control) × 100.

Percentage Inhibition of Edema (Carrageenan-Induced Paw Edema Method)

The anti-inflammatory activity of the test compounds was evaluated using the **carrageenan-induced paw edema model in rats,** a widely accepted experimental method for the assessment of acute inflammation.

Acute inflammation was induced by the **subplantar injection of carrageenan (1% w/v in normal saline, 0.1 mL)** into the right hind paw of each animal. The animals were divided into different groups consisting of a normal control group, a carrageenan control (disease control) group, test groups receiving the synthesized compounds at the dose of **50 mg/kg, p.o.,** and a standard group treated with **indomethacin (10 mg/kg, p.o.).** Test compounds and standard drug were administered orally **1 h prior to carrageenan injection.**

Paw volume was measured using a **plethysmometer** immediately before carrageenan administration (0 min) and at **1, 2, 3, 4, and 5 h** after carrageenan injection. The increase in paw volume was considered as edema and expressed as mean ± SEM.

The **percentage inhibition of edema** produced by the test compounds was calculated using the following formula:

Percentage Inhibition of Edema

Percentage Inhibition of Edema

$$\% \text{ Inhibition} = \frac{(E_c - E_t)}{E_c} \times 100$$

Where:

Ec = Mean edema of carrageenan control

Et = Mean edema of treated group

3. Results and Discussion

Physicochemical data of the synthesized compounds

The process described in the experimental section was followed in the synthesis of the various pyrrolidone derivatives. NMR and MS were used to determine the structure of the generated molecules.

Table 3. Physicochemical data of the synthesized compounds

COMPOUND CODE	R1	R2	R3	R4	R5	MOLECULAR FORMULA (M.W)	MP (°C)	YIELD (%)	Rf values
Compound 1	H	H	H	H	H	C28H26N2O5S (502.44)	201-203	52.12	0.21
Compound 2	H	H	H	Cl	H	C28H25ClN2O5S (536.31)	210-212	61.17	0.23
Compound 3	H	H	H	H	Cl_4	C28H25ClN2O5S (536.12)	215-217	57.21	0.22
Compound 4	H	H	H	NO_2	H	C28H25N3O7S (547.04)	199-202	50.12	0.24
Compound 5	H	H	H	H	NO_2	C28H25N3O7S (547.10)	212-214	62.17	0.25
Compound 6	H	H	H	Cl_4	H	C25H22ClN3O3S (479.10)	218-219	58.21	0.26
Compound 7	H	H	H	H	Cl_4	$C25H22Cl4N3O3S^{3+}$ (584.31)	235-237	59.35	0.26
Compound 8	H	H	H	H	NO_2	C25H22N4O5S (490.10)	235-237	60.12	0.28
Compound 9	H	H	H	NO_2	H	C25H22N4O5S (490.02)	212-214	54.44	0.33
Compound 10	H	H	H	H	CO_4 H	C25H23N3O7S (509.13)	220-222	61.10	0.17

Spectral characterization

A. NMR

Compound 1

1H NMR δ (d, J = 8.47, 7.93, 7.93, 7.70, 7.50, 7.29, 7.28, 7.27, 7.25, 7.23, 7.08 Hz), (s, J = 5.79, 5.75, 5.56, 4.94 Hz), (d, J = 2.83, 2.83, 2.60, 2.60, 1.65, 1.65, 1.64, 1.64 Hz).

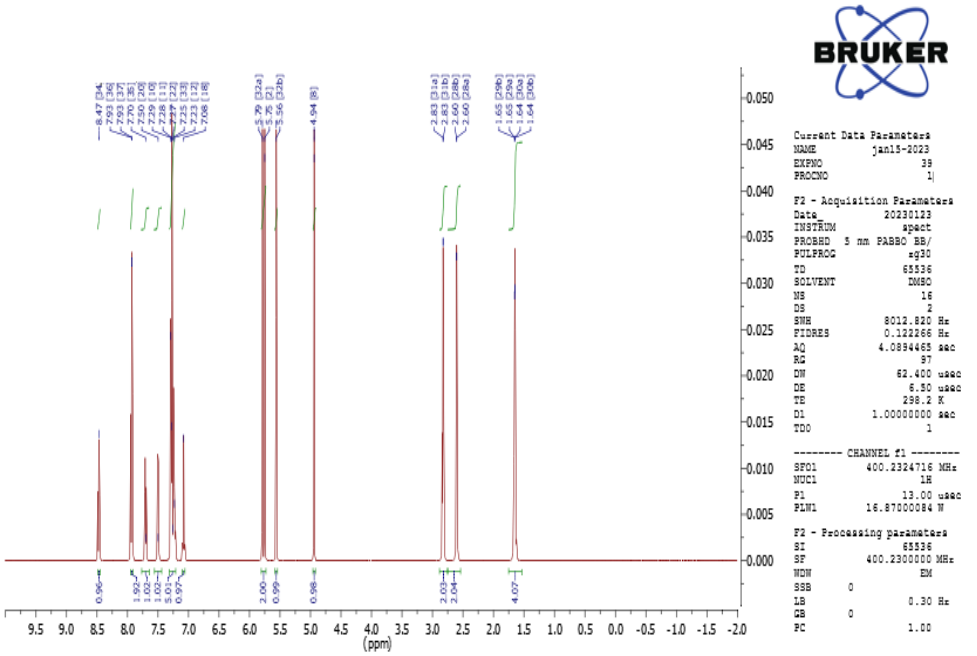

Figure 1. NMR Spectra of Compound 1

Compound 2

1H NMR δ (d, J = 8.58, 7.97, 7.97, 7.61, 7.50, 7.43, 7.07, 7.05, 7.02, 6.91 Hz), (s, J = 5.65, 5.55, 5.55, 3.87 Hz), (d, J = 2.83, 2.83, 2.60, 2.60, 1.66, 1.66, 1.64, 1.64 Hz).

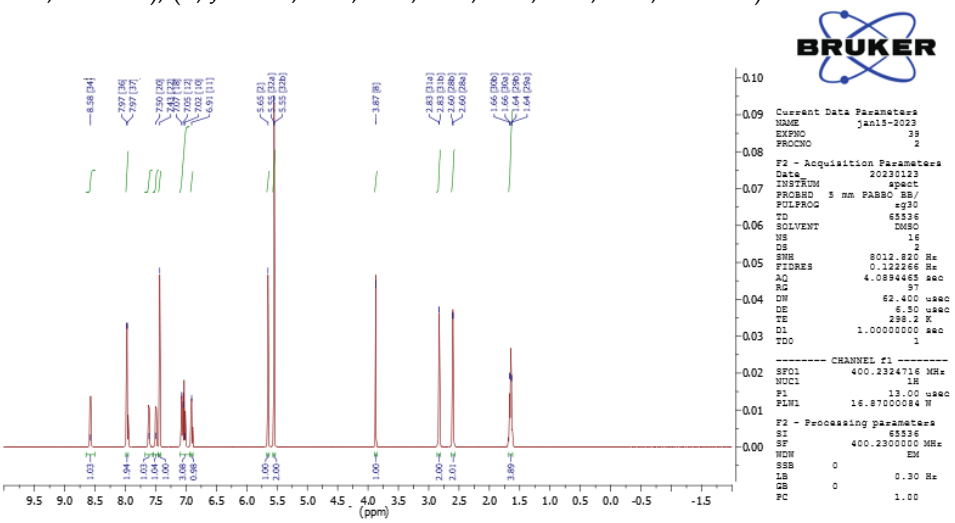

Figure 2. NMR Spectra of Compound 2

Compound 3

1H NMR δ (s, J = 8.91 Hz), (d, J = 7.67, 7.67, 7.58, 7.47 Hz), (m, J = 7.31, 7.24, 7.19, 7.08, 7.08 Hz), (d, J = 5.57, 5.57 Hz), (m, J = 5.36, 4.90, 2.83, 2.83, 2.61, 2.61, 1.67, 1.67, 1.67, 1.67 Hz).

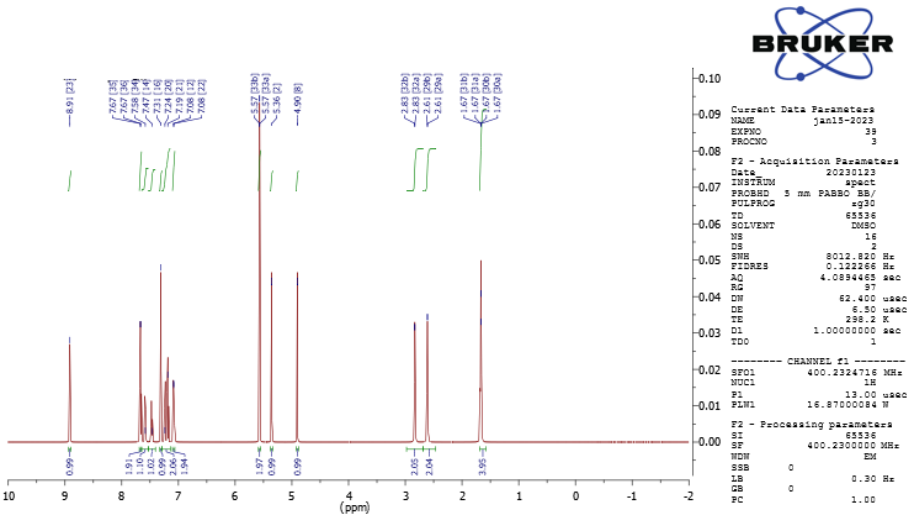

Figure 3. NMR Spectra of Compound 3

Compound 4

1H NMR δ (s, J = 9.61 Hz), (d, J = 8.01, 7.75, 7.75, 7.57, 7.52, 7.50, 7.48 Hz), (m, J = 7.34, 7.08 Hz), (d, J = 5.57, 5.57 Hz), (m, J = 5.49, 5.13, 2.83, 2.83, 2.61, 2.61, 1.67, 1.67, 1.67, 1.67 Hz).

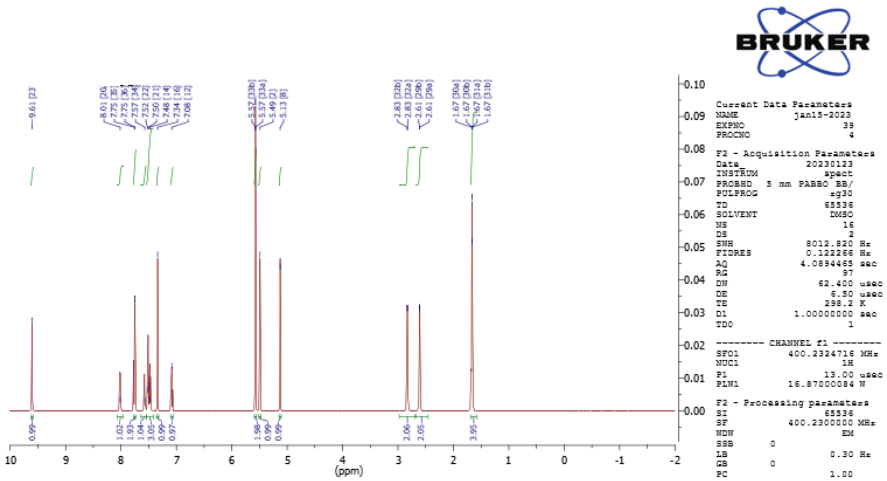

Figure 4. NMR Spectra of Compound 4

Compound 5

1H NMR δ (s, J = 9.61 Hz), (d, J = 8.01, 7.75, 7.75, 7.57, 7.52, 7.50, 7.48 Hz), (m, J = 7.34, 7.08 Hz), (d, J = 5.57, 5.57 Hz), (m, J = 5.49, 5.13, 2.83, 2.83, 2.61, 2.61, 1.67, 1.67, 1.67, 1.67 Hz).

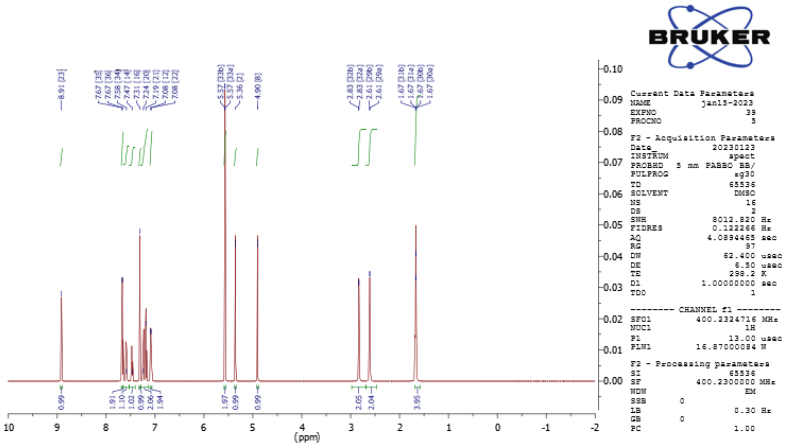

Figure 5. NMR Spectra of Compound 5

Compound 6

1H NMR δ (s, J = 8.87 Hz), (d, J = 7.85, 7.81, 7.58, 7.36 Hz), (m, J = 7.22, 7.18, 7.14, 7.12, 7.04, 6.06 Hz), (d, J = 5.80, 5.70 Hz), (m, J = 3.74, 2.83, 2.83, 2.60, 2.60, 1.66, 1.66, 1.66, 1.66 Hz).

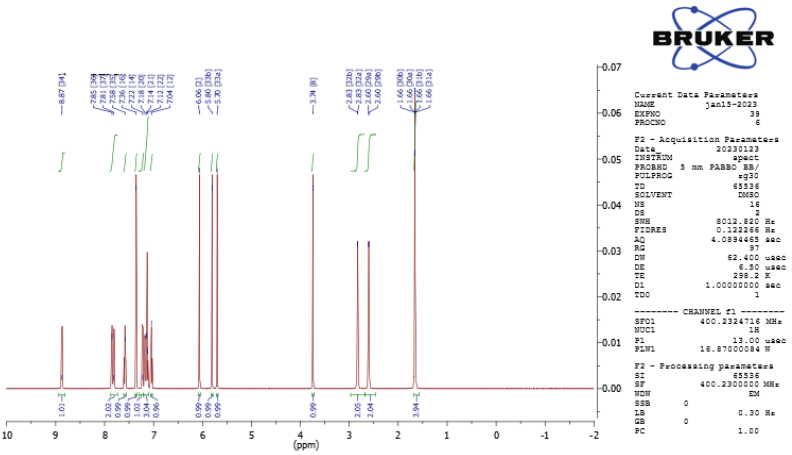

Figure 6. NMR Spectra of Compound 6

Compound 7

1H NMR δ (s, J = 8.87 Hz), (d, J = 7.85, 7.81, 7.58, 7.36 Hz), (m, J = 7.22, 7.18, 7.14, 7.12, 7.04, 6.06 Hz), (d, J = 5.80, 5.70 Hz), (m, J = 3.74, 2.83, 2.83, 2.60, 2.60, 1.66, 1.66, 1.66, 1.66 Hz).

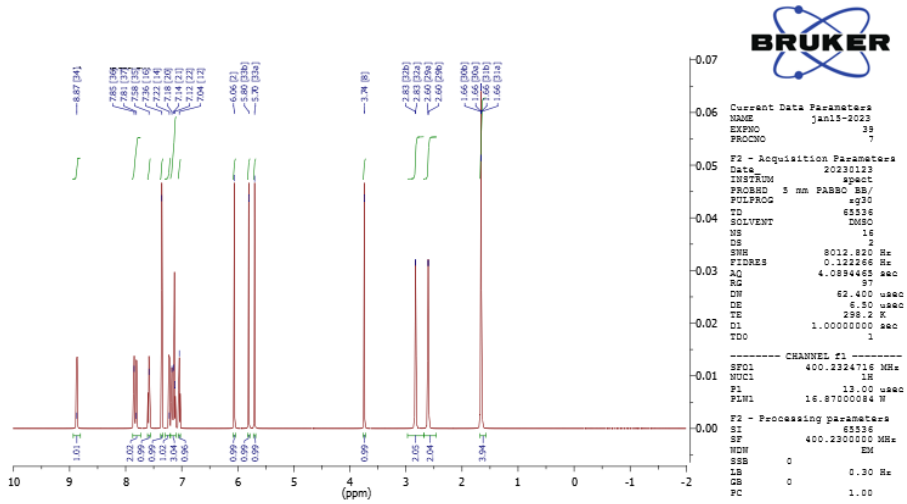

Figure 7. NMR Spectra of Compound 7

Compound 8

1H NMR δ (s, J = 9.61 Hz), (d, J = 8.01, 7.75, 7.75, 7.57, 7.52, 7.50, 7.48 Hz), (m, J = 7.34, 7.08 Hz), (d, J = 5.57, 5.57 Hz), (m, J = 5.49, 5.13, 2.83, 2.83, 2.61, 2.61, 1.67, 1.67, 1.67, 1.67 Hz).

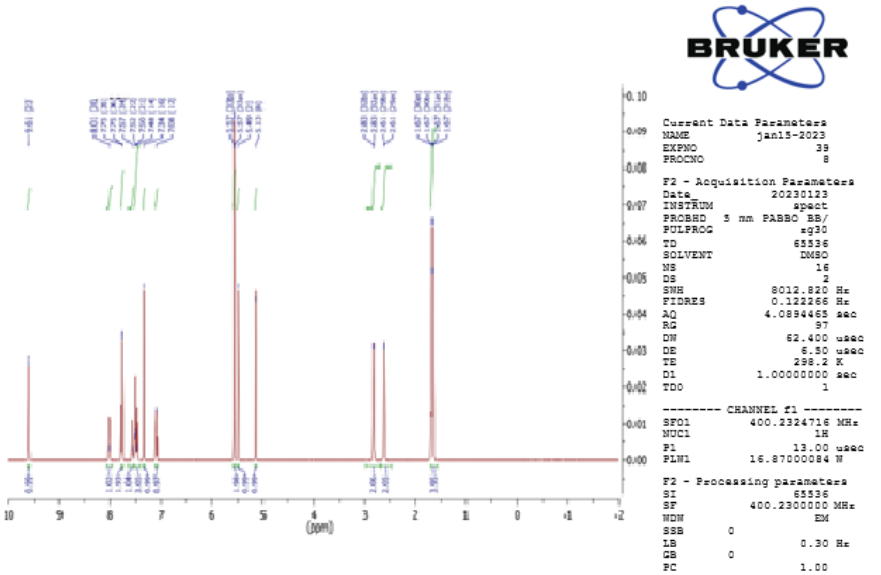

Figure 8. NMR Spectra of Compound 8

Compound 9

1H NMR δ (s, J = 9.61 Hz), (d, J = 8.01, 7.75, 7.75, 7.57, 7.52, 7.50, 7.48 Hz), (m, J = 7.34, 7.08 Hz), (d, J = 5.57, 5.57 Hz), (m, J = 5.49, 5.13, 2.83, 2.83, 2.61, 2.61, 1.67, 1.67, 1.67, 1.67 Hz).

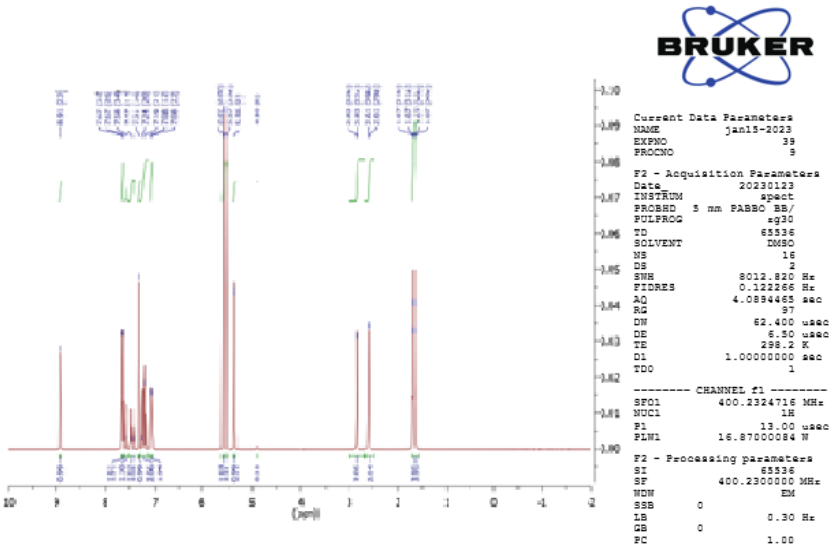

Figure 9. NMR Spectra of Compound 9

Compound 10

1H NMR δ (s, J = 12.78 Hz), (d, J = 7.79, 7.67, 7.45, 7.41 Hz), (m, J = 7.20, 7.10, 7.09, 7.06, 6.80, 6.74 Hz), (d, J = 5.56, 5.56 Hz), (m, J = 5.36, 4.63, 2.83, 2.83, 2.61, 2.61, 1.67, 1.67, 1.67, 1.67 Hz).

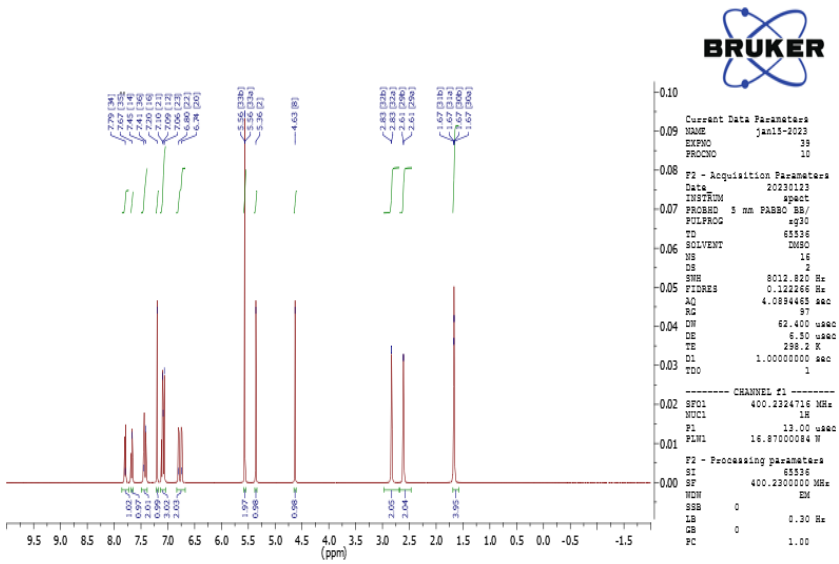

Figure 10. NMR Spectra of Compound 10

B. Mass Spectroscopy

Compound 1

The suggested structure with C28H26N2O5S matched the MS's molecular ion signal at m/z 502.44 (M] +). Thus, spectroscopic investigations led to the conclusion that chemical 1 may be classified as a pyrrolidone derivative.

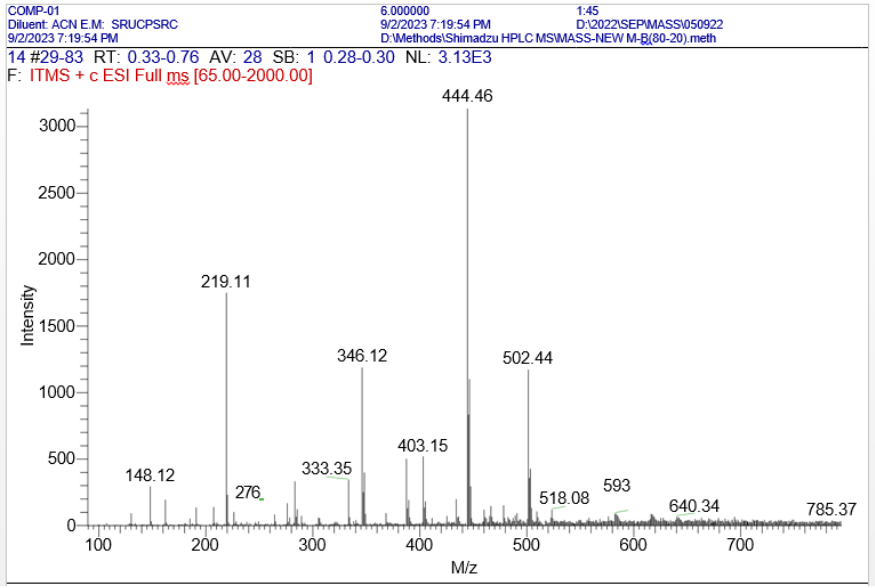

Figure 11. Mass Spectra of Compound 1

Compound 2

The suggested structure with C28H25ClN2O5S was consistent with the MS's molecular ion signal at m/z 536.31 (M] +). Thus, spectroscopic analysis led to the conclusion that chemical 2 may be classified as a pyrrolidone derivative.

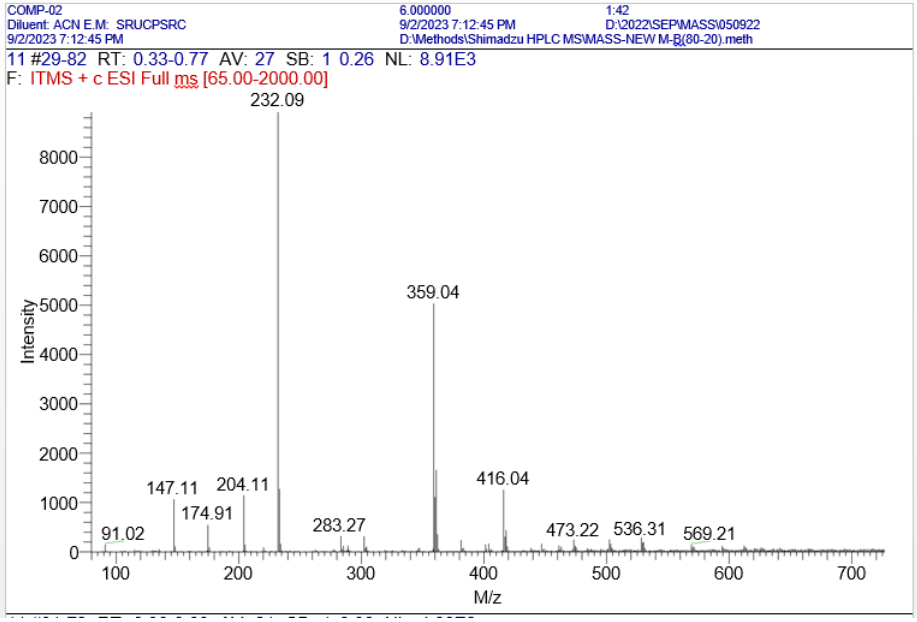

Figure 12. Mass Spectra of Compound 2

Compound 3

At m/z 536.12 (M] +, the MS displayed a molecular ion peak that matched the suggested structure with C28H25ClN2O5S. Thus, spectroscopic investigations led to the conclusion that chemical 3 may be classified as a pyrrolidone derivative.

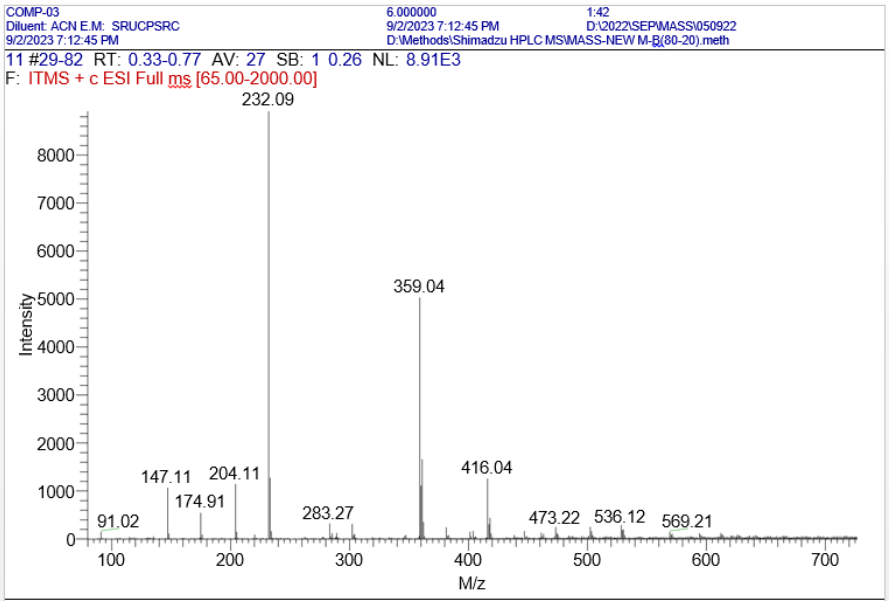

Figure 13. Mass Spectra of Compound 3

Compound 4

At m/z 547.40 (M] +, the MS revealed a molecular ion peak that matched the suggested structure with C28H25N3O7S. Thus, spectroscopic analysis led to the conclusion that chemical 4 may be classified as a pyrrolidone derivative.

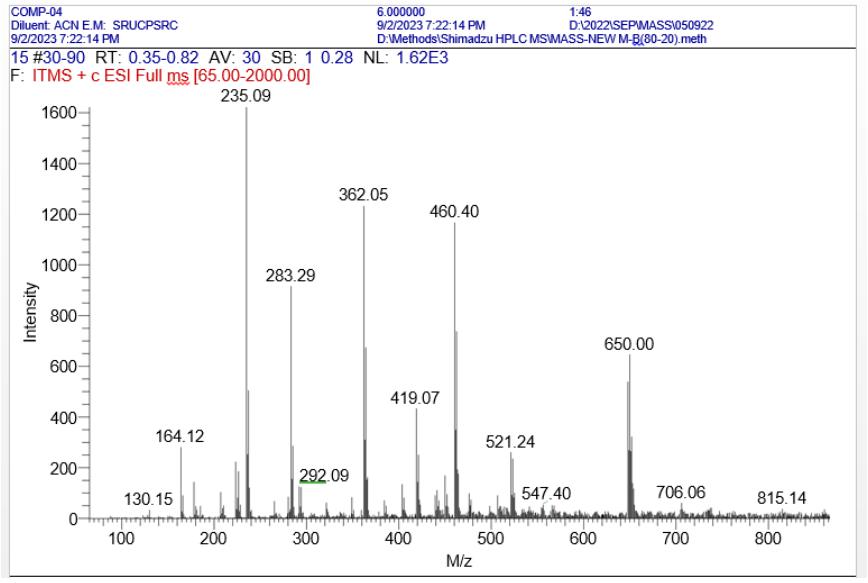

Figure 14. Mass Spectra of Compound 4

Compound 5

At m/z 547.10 (M] +, the MS revealed a molecular ion peak that matched the suggested structure of C28H25N3O7S. Thus, spectroscopic analysis led to the conclusion that chemical 5 may be classified as a pyrrolidone derivative.

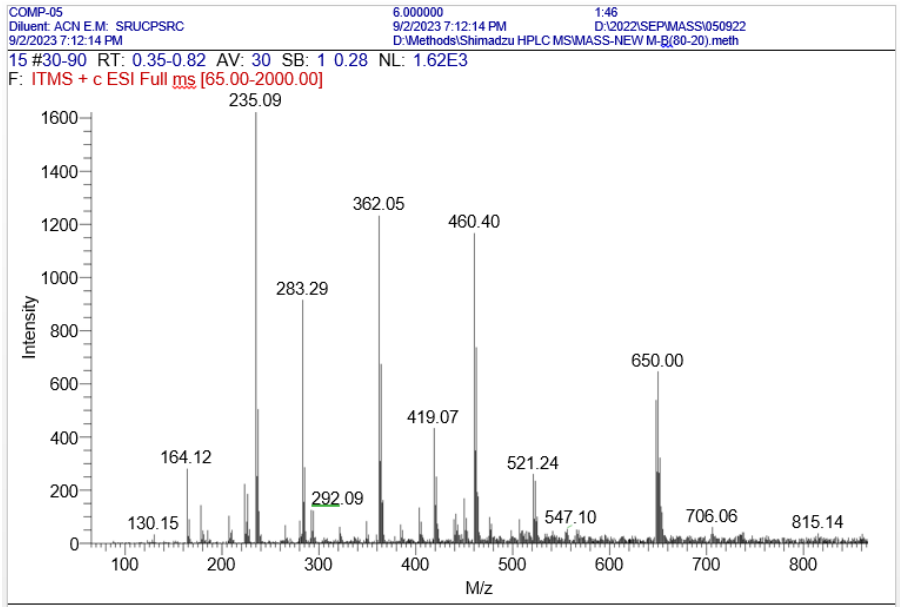

Figure 15. Mass Spectra of Compound 5

Compound 6

The MS showed a molecular ion peak at m/z 479.10 (M] + and was in match with the proposed structure with C25H22ClN3O3S. Thus, spectroscopic analyses led to the conclusion that chemical 6 may be classified as a pyrrolidone derivative.

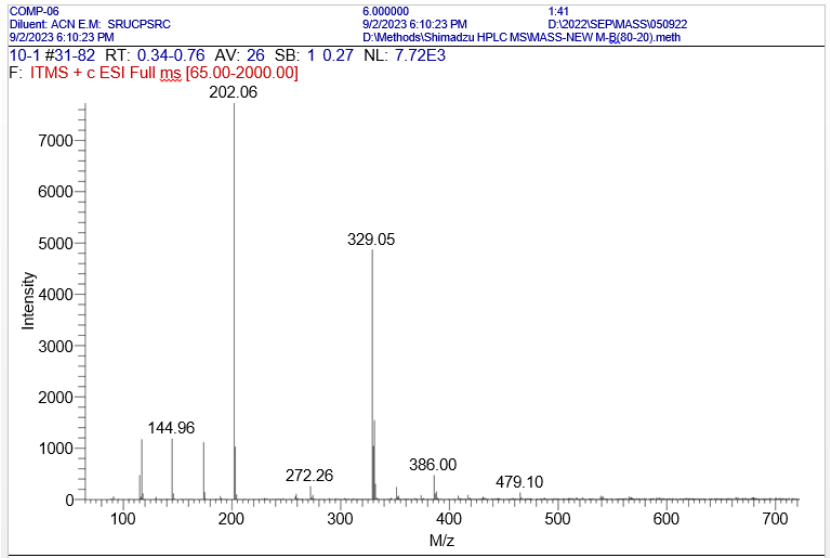

Figure 16. Mass Spectra of Compound 6

Compound 7

The suggested structure with C25H22Cl4N3O3S3+ matched the MS's molecular ion signal at m/z 584.31 (M] +). Thus, spectroscopic investigations led to the conclusion that chemical 7 may be classified as a pyrrolidone derivative.

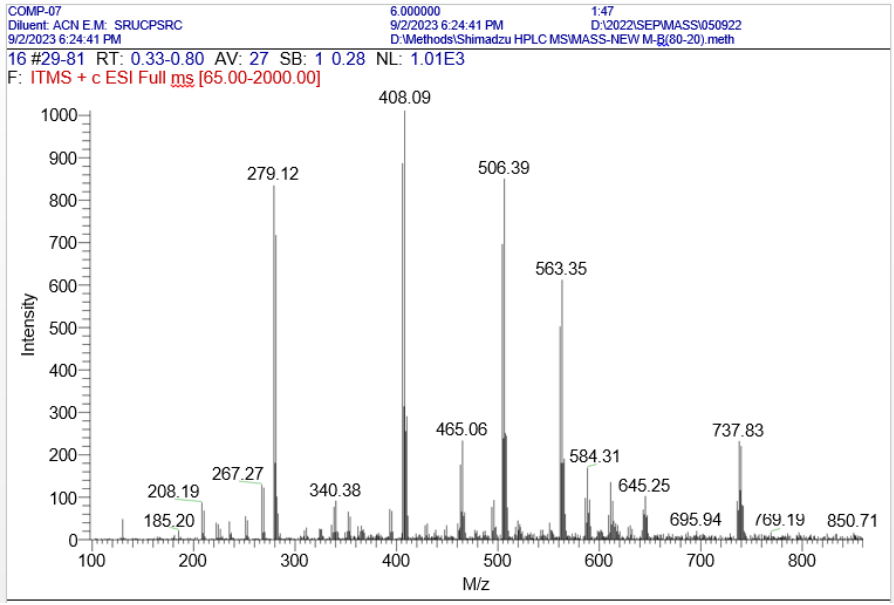

Figure 17. Mass Spectra of Compound 7

Compound 8

The MS revealed a molecular ion peak at m/z 490.10 (M] +, which matched the suggested structure with C25H22N4O5S. Thus, spectroscopic investigations led to the conclusion that chemical 8 may be classified as a pyrrolidone derivative.

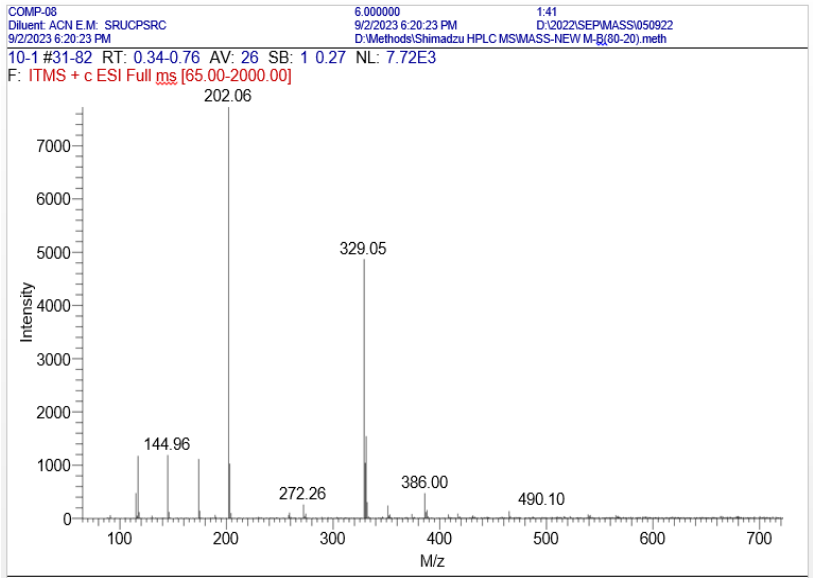

Figure 18. Mass Spectra of Compound 8

Compound 9

The suggested structure with C25H22N4O5S matched the MS's molecular ion signal at m/z 490.02 (M] +). Thus, spectroscopic investigations led to the conclusion that chemical 9 may be classified as a pyrrolidone derivative.

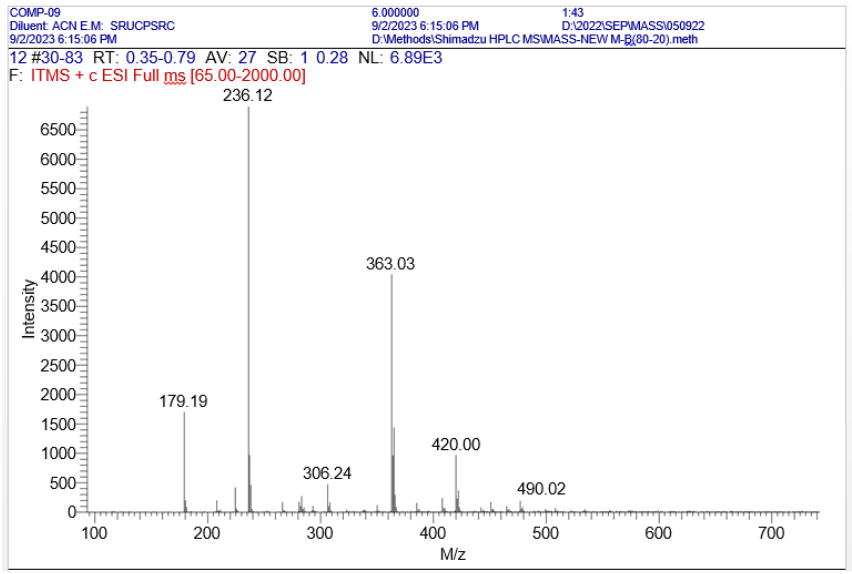

Figure 19. Mass Spectra of Compound 9

Compound 10

At m/z 509.13 [M] +, the MS revealed a molecular ion peak that matched the suggested structure with C25H23N3O7S. Thus, spectroscopic investigations led to the conclusion that chemical 10 may be classified as a pyrrolidone derivative.

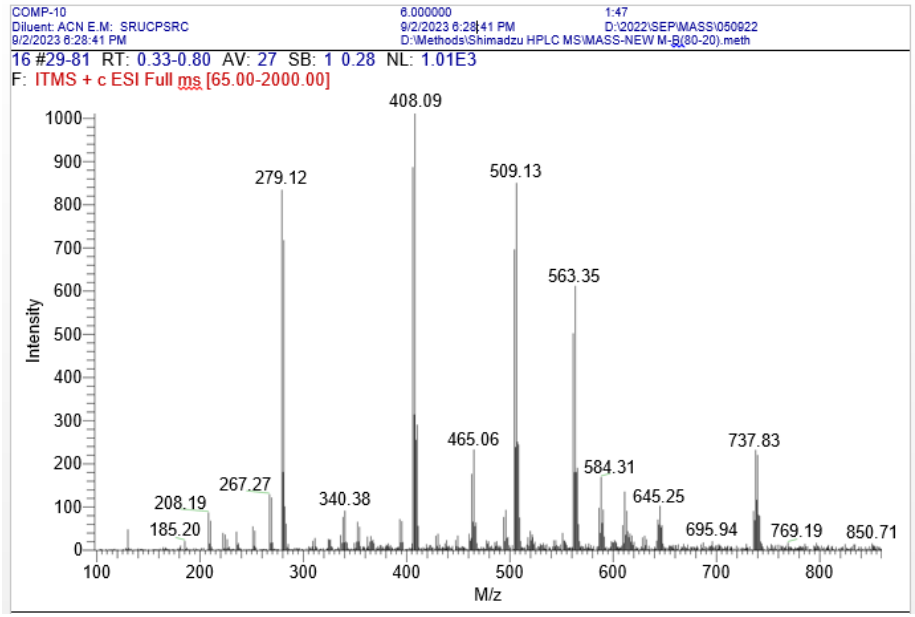

Figure 20. Mass Spectra of Compound 10

Biological Activity

Table 3. Effectofcompound 10 (C10) on hotplatetest:

Treatment	Responsetime(sec)				
	0h	0.5h	1h	2h	3h
Control(10ml/kg)	8.30±0.63	7.42±0.42	7.50±0.39	7.50±0.45	7.18±0.33
Standard(10mg/kg)	8.42±0.29	11.59±0.32**	13.58±0.38**	14.98±0.48***	16.38±0.27***
compound 10	8.27±0.32	10.25±0.31**c	10.94±0.13***a	11.27±0.58**a	11.98±0.37***b

Treatment	Responsetime(sec)				
	0h	0.5h	1h	2h	3h
(C10) (20mg/kg)					

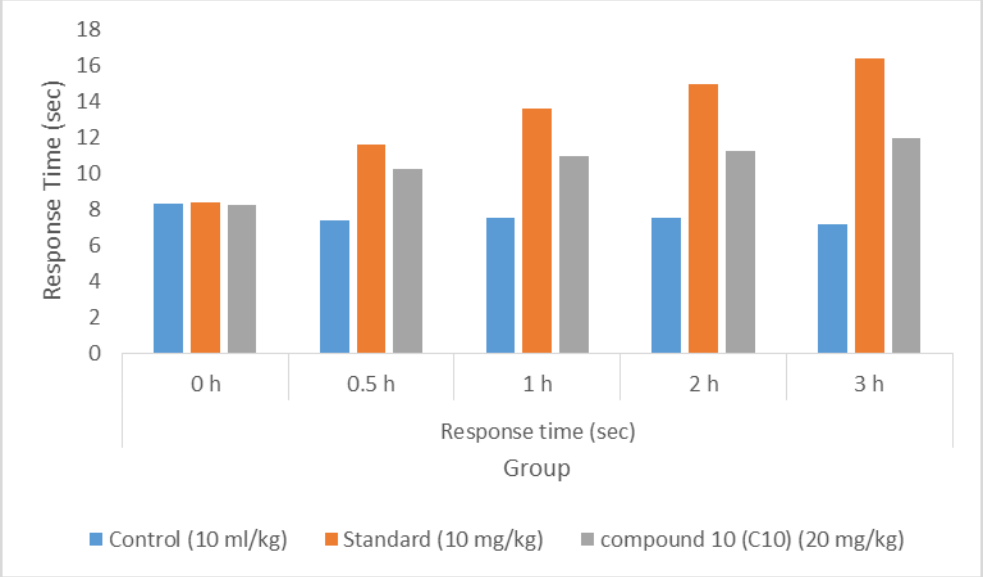

Figure 21. Effect of compound 10 in Hot Plate method

Values are expressed as mean ± SEM (standard error of the mean). Values were calculated using one-way ANOVA followed by Dunnett's test.* indicates $P < 0.001$ and ** indicates $P < 0.01$ when compared to the control. *a* indicates $P < 0.001$, *b* indicates $P < 0.01$, and *c* indicates $P < 0.05$ when compared to the standard drug. *p.o.*; $n = 6$.** The analgesic activity test using the hot plate method indicates that the control group shows consistent response times with minimal changes. The standard treatment (10 mg/kg) demonstrates a significant and continuous increase in response time over the 3-hour period, suggesting a strong analgesic effect. Similarly, the Compound 10 (C10) treatment (20 mg/kg) also results in a notable increase in response time, though to a slightly lesser extent than the standard treatment. Overall, both treatments exhibit significant analgesic properties, with the standard treatment having a more pronounced effect on response times compared to Compound 10.

Table 4. Effect of compound 10 (C10) on acetic acid induced writhing in mice

Treatment	Totalwrithingcount (Mean±SEM)	%Inhibition
Control	17.4±2.50	-
Standard	6.2±0.66***	64.36
Compound 10 (C10) (20mg/kg)	10.10±0.41**	41.95

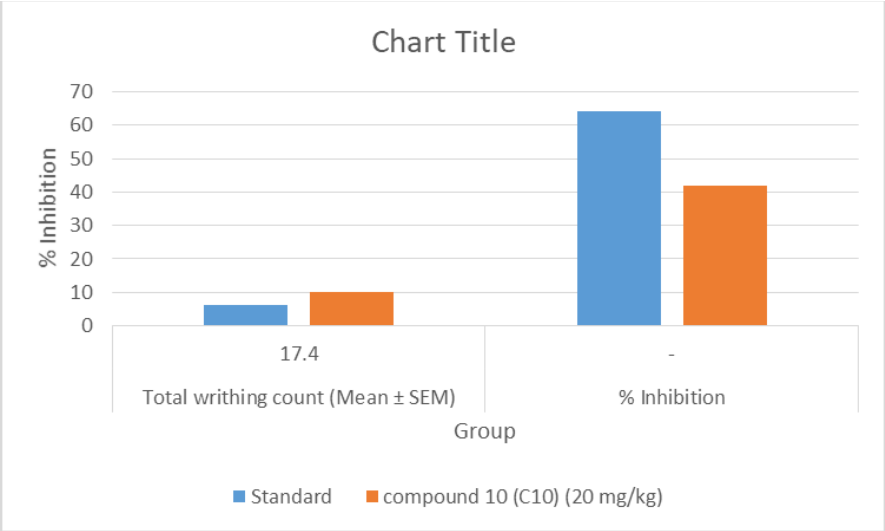

Figure 22. Effect of compound 10 (C10) on acetic acid induced writhing in mice

Values are expressed as mean ± SEM (standard error of the mean). Values were calculated using one-way ANOVA followed by Dunnett's test. *** indicates $P < 0.001$ and ** indicates $P < 0.01$ when compared to the control. a indicates $P < 0.001$, b indicates $P < 0.01$, and c indicates $P < 0.05$ when compared to the standard drug. p.o.; n = 6. The data on total writhing count suggests notable analgesic effects for both the standard treatment and Compound 10 (C10). The control group has a mean writhing count of 17.4 ± 2.50, serving as the baseline with no inhibition. The standard treatment significantly reduces the writhing count to 6.2 ± 0.66, representing a 64.36% inhibition, indicating a strong analgesic effect. Similarly, Compound 10 (C10) at 20 mg/kg shows a reduction in writhing count to 10.10 ± 0.41, resulting in a 41.95% inhibition, demonstrating considerable analgesic activity though slightly less pronounced than the standard treatment. These results underscore the efficacy of both treatments in reducing pain responses.

Table 5. Effect of compound 10 (C10) on Carrageenan-Induced Paw Edema

Sr. No	**Group / Treatment**	**0 min**	**1 h**	**2 h**	**3 h**	**4 h**	**5 h**
1	**Normal Control**	0.24 ± 0.01 NS	0.24 ± 0.01 NS	0.25 ± 0.01 NS	0.25 ± 0.01 NS	0.25 ± 0.01 NS	0.26 ± 0.01 NS
2	**Disease Control (1% Tween 80, p.o.)**	0.24 ± 0.01 NS	0.38 ± 0.02 NS	0.49 ± 0.02 NS	0.63 ± 0.03 NS	0.72 ± 0.02 NS	0.75 ± 0.03 NS
3	**Standard Indomethacin (10 mg/kg)**	0.25 ± 0.02 NS	0.28 ± 0.02**	0.30 ± 0.02**	0.32 ± 0.02**	0.33 ± 0.02 **	0.34 ± 0.02**
4	**Compound 10 (10 mg/kg)**	0.24 ± 0.02 NS	0.32 ± 0.02**	0.36 ± 0.02**	0.41 ± 0.02**	0.45 ± 0.02 **	0.48 ± 0.02**

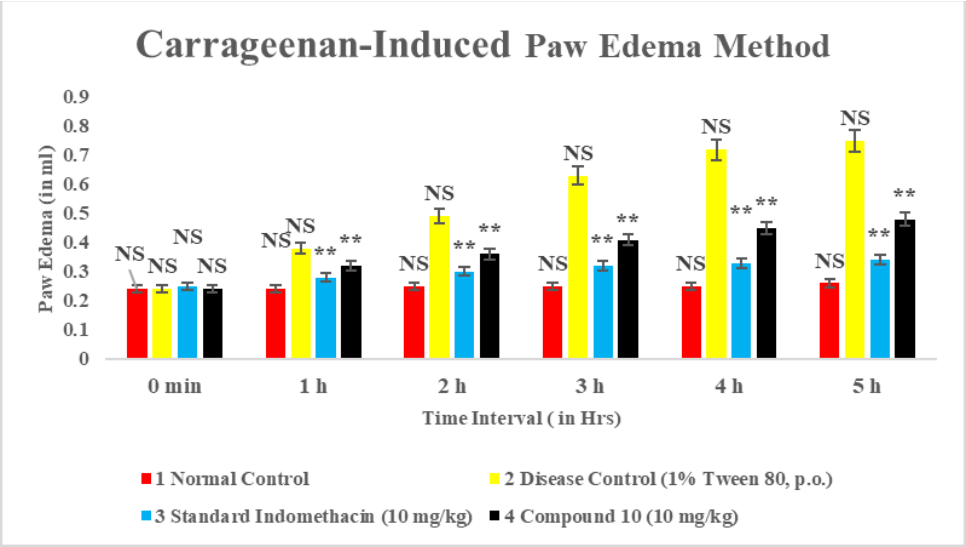

Figure 23. Effect of compound 10 (C10) on Carrageenan-Induced Paw Edema in mice

Values are expressed as mean ± SEM (standard error of the mean). Values were calculated using one-way ANOVA followed by Dunnett's test. *** indicates $P < 0.001$ and ** indicates $P < 0.01$ when compared to the control; *a* indicates $P < 0.001$, *b* indicates $P < 0.01$, and *c* indicates $P < 0.05$ when compared to the standard drug. p.o.; n = 6.

The present study demonstrates that **Compound 10 (10 mg/kg)**exhibits **significant anti-inflammatory activity** in the carrageenan-induced paw edema model. The **disease control group** showed a progressive and marked increase in paw volume from 1 to 5 h, confirming successful induction of acute inflammation. In contrast, the **normal control group** maintained a nearly constant paw volume throughout the experimental period.Treatment with the **standard drug Indomethacin (10 mg/kg)** produced a **significant (P < 0.01) reduction in paw edema** from the 1st hour onward, validating the sensitivity of the experimental model. Similarly, **Compound 10 (10 mg/kg)** significantly suppressed paw edema at all post-carrageenan time points (1–5 h) when compared with the disease control group.Although the inhibitory effect of Compound 10 was **less pronounced than Indomethacin**, it showed a **consistent and time-dependent reduction of inflammation,** particularly during the late phase (3–5 h), which is mainly mediated by prostaglandins. These findings suggest that **Compound 10 possesses appreciable anti-inflammatory potential,** possibly through inhibition of inflammatory mediators involved in the acute inflammatory response.Overall, the results indicate that **Compound 10 may serve as a promising lead compound for further anti-inflammatory drug development,** warranting additional mechanistic and dose-dependent studies.

4. Conclusion

This study's approach, which was inexpensive, highly selective, and simple to prepare, worked well. Additionally, it permits numerous stages of re-stimulation without causing damage to the stimulator. Since enormous amounts are not required, even a modest quantity of the stimulator can produce effective effects. Spectroscopic tests, including mass spectrometry and magnetic resonance spectroscopy, supported the study's conclusions and verified the manufactured goods' correctness. When compared to the primary antagonist, the compounds showed considerable effectiveness in reducing pain. Even at concentrations up to three times lower than the primary antagonist, compound C10 offered the greatest pain alleviation, almost half that of the latter. This implies that these substances may serve as antagonists in the future, saving money and time.

REFERENCES

[1] C. Shultz, V. Nair, J. Hong *et al.*, "Pyrrolidone-based compounds as potential therapeutic agents: A review," *J. Med. Chem.*, vol. 60, no. 15, pp. 6615–6644, 2017.
[2] S. Singh, A. Sharma, and P. Dhingra, "Recent developments in pyrrolidone derivatives and their biological activities," *Bioorg. Med. Chem. Lett.*, vol. 25, no. 9, pp. 1966–1976, 2015.
[3] J. Barros, M. Bastos, and A. Carvalho, "Applications of iodine as a catalyst in organic synthesis: A review," *J. Org. Chem.*, vol. 84, no. 13, pp. 7517–7533, 2019.
[4] M. Silva, C. Andrade, and P. Carvalho, "Iodine-catalyzed cyclization reactions: Applications in the synthesis of heterocyclic compounds," *Chem. Rev.*, vol. 120, no. 2, pp. 727–756, 2020.
[5] V. Pande and V. Gupta, "Functionalized pyrrolidones and their applications in medicinal chemistry: A comprehensive review," *Future Med. Chem.*, vol. 12, no. 5, pp. 375–397, 2020.
[6] D. A. Evans and D. Seidel, "Catalysis in organic synthesis: A green approach to sustainable chemistry," *J. Am. Chem. Soc.*, vol. 140, no. 19, pp. 6294–6306, 2018.
[7] P. Rao and M. Reddy, "Advances in the synthesis and functionalization of pyrrolidone derivatives for drug discovery," *Med. Chem. Res.*, vol. 25, no. 7, pp. 1210–1224, 2016.
[8] D. McNeal, T. Lohrmann, and D. Williams, "Green catalysis and the role of iodine in organic reactions," *ChemSusChem*, vol. 10, no. 6, pp. 1253–1264, 2017.
[9] M. Rawat and M. Patel, "Anticancer and anti-inflammatory potential of pyrrolidone derivatives: An overview of recent advancements," *J. Enzyme Inhib. Med. Chem.*, vol. 33, no. 1, pp. 238–250, 2018.
[10] H. Wang, Y. Lee, and Y. Zhang, "Pyrrolidone derivatives: Synthesis and biological evaluations," *Pharmaceutics*, vol. 10, no. 4, p. 215, 2018.
[11] M. Ochoa-Villarreal, L. Garcia-Ruiz, V. Chavez-Avila *et al.*, "Pyrrolidone derivatives: Recent advances in their synthesis and pharmacological activities," *Eur. J. Med. Chem.*, vol. 174, pp. 85–101, 2019.
[12] A. Kumar, N. Yadav, A. Yadav *et al.*, "Design, synthesis, and biological evaluation of novel pyrrolidone derivatives as potential antimicrobial agents," *Med. Chem. Res.*, vol. 30, no. 3, pp. 431–441, 2021.
[13] M. Pinto, C. Amorim, D. Fonseca *et al.*, "The role of iodine in organic synthesis: Mechanisms and applications in green chemistry," *Chem. Soc. Rev.*, vol. 47, no. 19, pp. 7252–7287, 2018.
[14] S. Singla, V. Kapoor, S. Singh *et al.*, "Development of novel pyrrolidone derivatives: Synthesis, biological activities, and structure-activity relationships," *Bioorg. Med. Chem.*, vol. 24, no. 12, pp. 2962–2977, 2016.
[15] S. Subramanian and P. Sundararajan, "Iodine-catalyzed heterocyclic synthesis: A green approach for sustainable development," *Org. Biomol. Chem.*, vol. 18, no. 5, pp. 748–767, 2020.
[16] K. Patel, S. Dighe, D. Jadhav *et al.*, "Iodine-catalyzed functionalization of pyrrolidone derivatives: Applications in medicinal chemistry," *Tetrahedron Lett.*, vol. 58, no. 24, pp. 2289–2294, 2017.
[17] Y. Li, Q. Zhao, Z. Tan *et al.*, "Synthesis and biological evaluation of pyrrolidone-based compounds as anti-inflammatory agents," *J. Pharm. Sci.*, vol. 108, no. 10, pp. 3245–3253, 2019.
[18] S. Mohapatra, N. Sahu, D. Rathore *et al.*, "Anticancer activity of pyrrolidone derivatives: A comprehensive review," *Pharmacol. Res.*, vol. 128, pp. 105–122, 2018.
[19] Q. Zhang, C. Liu, S. Liu *et al.*, "The impact of iodine catalysis in the synthesis of heterocyclic compounds with bioactive properties," *Adv. Synth. Catal.*, vol. 362, no. 8, pp. 1783–1801, 2020.
[20] Y. Cheng, J. Liu, and W. Zhang, "Synthesis and characterization of new pyrrolidone derivatives using iodine as a catalyst for potential therapeutic applications," *RSC Adv.*, vol. 10, no. 4, pp. 2300–2310, 2020.
[21] S. Yu, H. Liu, M. Li *et al.*, "Recent advances in ultrasound-assisted organic synthesis," *Ultrason. Sonochem.*, vol. 31, pp. 191–210, 2016.
[22] S. Zhang, Z. Sun, J. Xie *et al.*, "Diethyl acetylenedicarboxylate as a reagent for synthesis of conjugated derivatives in organic reactions," *Tetrahedron Lett.*, vol. 58, no. 2, pp. 163–167, 2017.
[23] R. Kumar, S. Sharma, V. Bansal *et al.*, "Citric acid-catalyzed synthesis of bioactive compounds in organic reactions: A review," *J. Mol. Catal. A Chem.*, vol. 429, pp. 1–13, 2017.
[24] V. Singh, M. Kumar, and S. Singh, "Sonochemistry in organic synthesis: Recent applications and advancements," *Ultrason. Sonochem.*, vol. 47, pp. 22–34, 2018.
[25] K. Balakrishnan, S. T. Selvan, M. Rani *et al.*, "Sonochemical synthesis of novel organic compounds and their evaluation for biological activity," *Chem. Pharm. Bull.*, vol. 67, no. 1, pp. 34–42, 2019.
[26] S. Hunskaar, O. B. Fasmer, J. Senn *et al.*, "The hot plate test: A reappraisal of its use in the screening of analgesics," *J. Pharmacol. Methods*, vol. 14, no. 3, pp. 221–226, 1985.

[27] R. P. Babu, P. Selvakumar, S. Muralidharan *et al.*, "Analgesic and anti-inflammatory activities of the ethanol extract of the root of *Withania somnifera* (L.) Dunal," *J. Ethnopharmacol.*, vol. 124, no. 3, pp. 455–458, 2009.